Presented at the SLAC Topical Conference 7/10-21/78
Proceedings of the Summer Institute on Particle Physics

BNL-24932
OG432

MASTER

Conf. 780769--4

Recent Results from the FNAL 15 Foot Bubble Chamber

M.J. Murtagh

Physics Department, Brookhaven National Laboratory

DISCLAIMER

Presented at the SLAC Topical Conference 7/10-21/78

Recent Results from the FNAL 15 Foot Bubble Chamber

M.J. Murtagh

TABLE OF CONTENTS

Recent Results from the FNAL 15 Foot Bubble Chamber

M.J. Murtagh
Physics Department, Brookhaven National Laboratory

I. Introduction

Recent results from the Fermilab 15' Bubble Chamber on charm production by neutrinos and antineutrinos and on the measurement of the elastic scattering of muon neutrinos on electrons are discussed. All the results come from exposures of the chamber filled with a heavy neon-hydrogen (64% at. neon) mixture. In this liquid electrons are easily identified through visible bremmstrahlung since the radiation length is only 40 cms. With any reasonably defined fiducial volume and the requirement that electrons are identified by at least two signatures, the detection efficiency for electrons is $\gtrsim$ 85%. The interaction length for hadrons is 125 cms, so that hadrons typically interact while muons leave the chamber without interacting and can, in general, be identified on the scan table. From the comparison of interacting and non-interacting tracks of both signs the background of fake μ^- from hadron punchthrough is estimated to be about 10%.

The neutrino results presented (unless otherwise stated) are from the Brookhaven National Laboratory-Columbia University experiment (Exp. 53A).[1] The total exposure of 134,000 pictures contains 106,000 charged current neutrino interactions. The present dilepton ($\mu^- e^+$) sample which is double the published data from this experiment[2] is clearly consistent with the GIM charm model. In addition, the non-leptonic

charm decay $K^{o}\pi^{+}\pi^{-}$ of the D^{o} has been observed.[3] The current status of the search for charmed baryons is presented.

The cross-section for $\nu_{\mu} - e^{-}$ elastic scattering has been measured.[4] When analyzed in terms of the Weinberg-Salam model this result yields a value of $\sin^{2}\theta_{w} = 0.2$ which is consistent with the value obtained from neutrino hadron scattering. This is in contrast to the recent GARGAMELLE results[5] which gave a Weinberg-Salam angle $\sin^{2}\theta_{w} \sim 0.73$.

Recently two groups[6,7] have reported on dilepton ($\mu^{+}e^{-}$) production by antineutrinos. While the number of events is still small, the results are clearly consistent with the expectations of the GIM model.

II. Charm Production

Dilepton production by neutrinos was first reported almost four years ago.[8] Since then many arguments have been advanced as to why dilepton events are manifestations of GIM charm production.[9] However, these counter experiments were unable to investigate one of the basic premises of the GIM scheme; the strong correlation between charm and strangeness. This information is the province of bubble chambers and the current situation on the strange particle content of dilepton events will be emphasized in the following discussion.

a) By Neutrinos

Charm particles[10] can be produced in charged current neutrino interactions either by interactions on d quarks or on s quarks in the $s\bar{s}$ sea.

Valence:

$d(x)\sin^2\theta_c$

1 S.P. per event

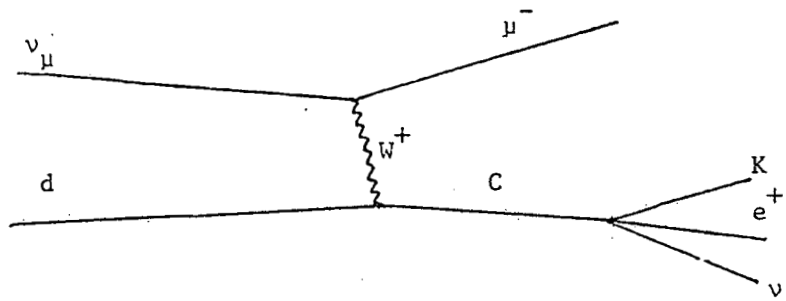

Sea:

$s(x)\cos^2\theta_c$

2 S.P. per event

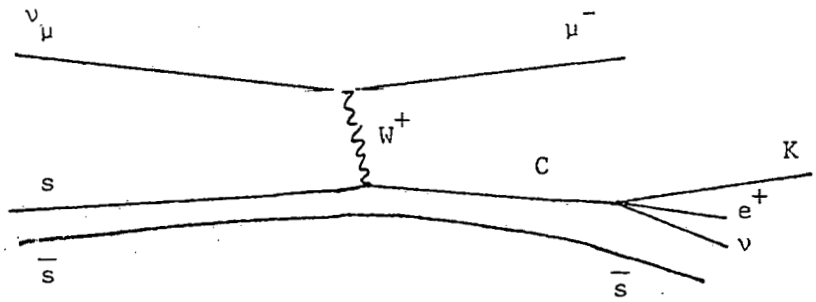

When they decay semileptonically, e^+ particles are produced. Thus, one expects to find $\mu^- e^+$ events. In charm production from valence quarks, the total charm production rate is $\sin^2\theta_c$ (5%), where θ_c is the Cabibbo angle. Since charm couples preferentially to strangeness, one expects one strange particle per event. In charm production from $s\bar{s}$ pairs in the sea, the production rate is $\sim s(x)\cos^2\theta_c$, where s(x) is the probability of finding an s quark with fractional momentum x. Here one expects $\sim$ two strange particles per event (one from the decay of c, the other from the leftover $\bar{s}$). These two mechanisms may have comparable rates. They can be distinguished by their characteristic x- distributions. The production on s quarks is expected to have a distribution peaked at small x, while production on a valence quark has a broader x distribution. In addition, the total strange particle content should be between one and two strange particles per event depending on the mixture of valence

and sea production.

b) By Antineutrinos

Antineutrinos can produce only anti-charm particles[10] either by interactions on $\bar{d}$ or $\bar{s}$ quarks in the sea.

Sea:
$d(x)\sin^2\theta_c$
1 S.P. per event

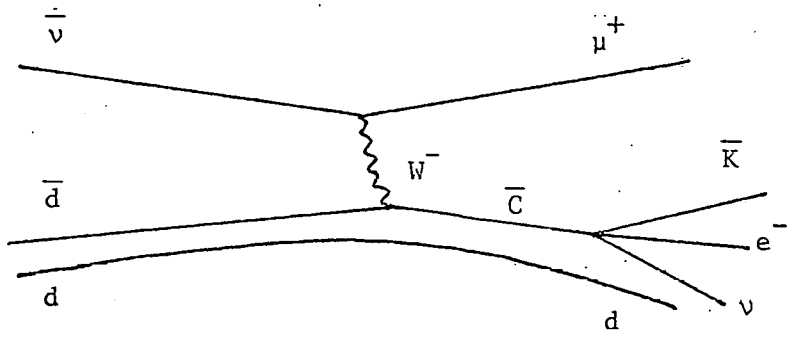

Sea:
$s(x)\cos^2\theta_c$
2 S.P. per event

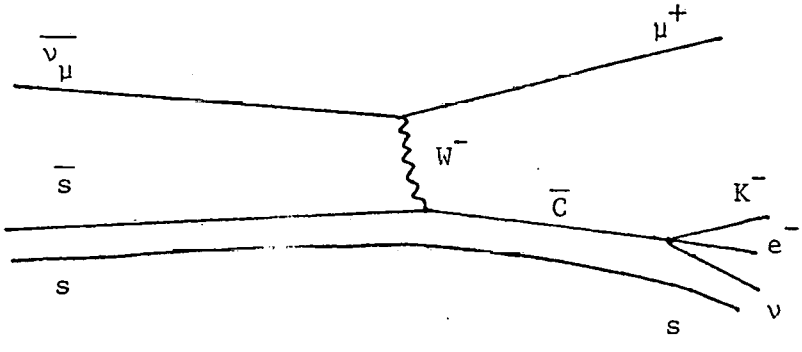

Since the production is always from sea quarks, the production from $\bar{s}$ should dominate since its rate is proportional to $\cos^2\theta_c$. Consequently, one expects antineutrinos to give μ^+e^- events with a characteristic "sea" x-distribution and approximately two strange particles per event.

III. Dilepton Production

a) By Neutrinos

A total of 164 events with at least a μ^- and an e^+ in the final state have been found in the analysis of 100,000 pictures,

corresponding to 60,000 charged current neutrino interactions. The e^+ is required to have two signatures and a momentum over 300 MeV/c. With these cuts, the background from asymmetric Dalitz pairs is a few percent. The μ^- is identified as the fastest negative leaving track. No momentum cut is made. From a comparison of interacting and noninteracting tracks of both signs, the background due to fake μ^- (hadron punchthrough) is determined to be about 10%. After correcting for these backgrounds, scan efficiency (~90%), and e^+ identification efficiency (~85%), the calculated dilepton rate is

$$R = \frac{\nu_\mu + Ne \rightarrow \mu^- + e^+ + \ldots}{\nu_\mu + Ne \rightarrow \mu^- + \ldots} = (0.5 \pm 0.15)\%.$$

This rate is calculated for half of the events for which there is an accurate normalization. Figure 1 shows the momentum distribution of the e^+, the μ^- and the total visible energy.

Various opening angles between selected particles as projected on the plane perpendicular to the beam direction are shown in Fig. 2. In general, one expects these angles to be shifted toward 0° for particles coming from the same production vertex and 180° for those particles emitted at opposite vertices. These results are consistent with the premise that the e^+ is associated with the hadron rather than the lepton vertex.

The 164 $\mu^- e^+$ events were examined for associated $K_S \rightarrow \pi^+\pi^-$ and $\Lambda \rightarrow p\pi^-$ decays. A total of 33 such vees (25 events with a single vee, 4 with a double vee) were found. After resolving the K^o/Λ ambiguities (10 of the 33 vees were ambiguous) there were 23 K^o_S and 10 Λ decays. This corresponds to 0.6 ± 0.2 neutral strange

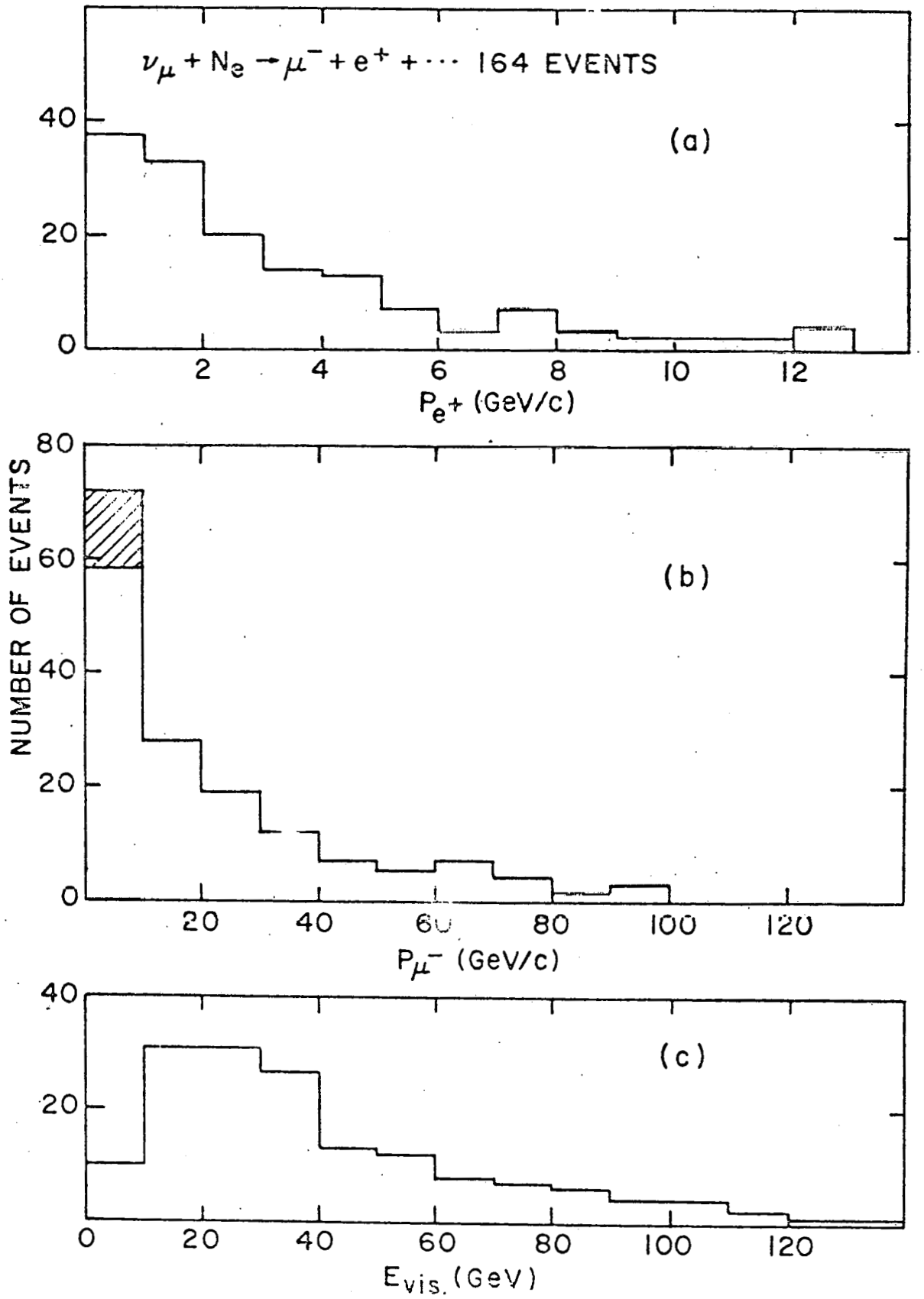

Fig. 1 Momentum of a) the e^+; and b) the μ^-, in the dilepton sample. The shaded events are the background from hadron punchthrough; c) the total visible energy.

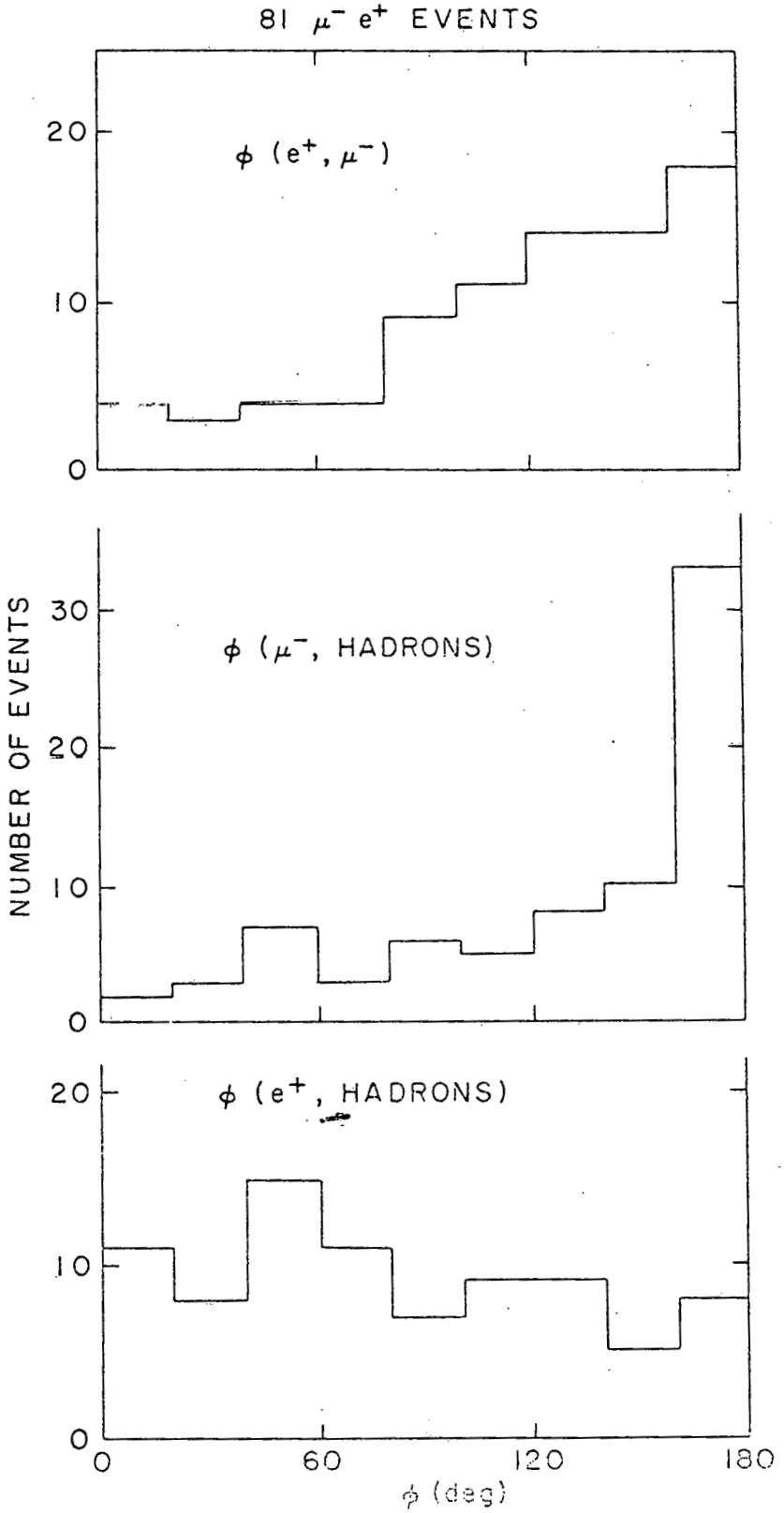

Fig. 2 Opening angles as projected onto the plane normal to the ν_μ beam direction.

particles per dilepton event. The visible vee production rate in normal charged current interactions is measured to be 6%. Therefore, one expects only 10 vees in 164 events, whereas 33 are observed. This excess of strange particles in dilepton events is as expected in the GIM charm model. Recently a number of other bubble chamber experiments have reported the observation of dilepton events in neutrino interactions (Table I, Fig. 3). Both the rate for dilepton production and the number of neutral strange particles per event are consistent with the results of the Brookhaven National Laboratory-Columbia University experiment.

The x distribution for the 164 $\mu^- e^+$ events (Fig. 4) can be fit to a mixture of the x distributions measured at SLAC and GARGAMELLE for valence and sea quarks. The best fit indicates that charm production by neutrinos is about 2/3 from valence and 1/3 from sea quarks. This ratio between charm production on valence and sea quarks implies that the sea s quark content is 3% of the valence d quark content in a neon target. The number of strange particles expected per event is, therefore, (2/3 x 1 strange particle) + (1/3 x 2 strange particles) = 1.33. On the assumption that charged and neutral strange particles are equally likely in charm decay, the observed total strange particle production rate is $\sim$1.2 strange particles per event.

The characteristics of these dilepton events strongly supports the conjecture that they are predominantly from the decay of charmed particles.

Figure 5 shows the $K^o e^+$ effective mass from the 19 $\mu^- e^+$ events

TABLE I

$\mu^- e^+$ From Other Experiments

Experiment	$\langle E_\nu \rangle$ BeV	Liquid	Events Observed	Vees* Observed	$\mu^- e^+/\mu^-$ Rate (%)
Gargamelle (11) CERN PS	1-8	Freon	14 $\mu^- e^+$	3	
Wisconsin-CERN-Hawaii-Berkeley (12) Fermilab 15 foot B.C., E28	∿30	21% Ne	17 $\mu^- e^+$	11	0.8 ± 0.3
Columbia-Brookhaven Fermilab 15 foot B.C., E53	∿30	64% Ne	164 $\mu^- e^+$	33	0.5 ± 0.15
Berkeley-Seattle-LBL-Hawaii (6) Fermilab 15 foot B.C., E172	∿30	64% Ne	6 $\mu^- e^+$	1	$0.34 \begin{smallmatrix} + 0.23 \\ - 0.13 \end{smallmatrix}$
Fermilab-LBL-Hawaii (13) Fermilab 15 foot B.C., E546	∿30	50% Ne	40 $\mu^- \mu^+$	5	0.43 ± 0.16
BEBC Narrow band (14) CERN SPS	∿75	60% Ne	11 $\mu^- \mu^+$ 5 $\mu^- e^+$	6 2	0.7 ± 0.3
BEBC Wide band (15) CERN SPS	∿30	60% Ne	21 $\mu^- e^+$	6	0.5 ± 0.17
GARGAMELLE Wide band (16) CERN SPS	∿30	Freon Propane	46 $\mu^- \mu^+$	6	0.7 ± 0.2

*Vees stand for $K_s^o \to \pi^+ + \pi^-$ or $\Lambda^o \to p + \pi^-$ decays

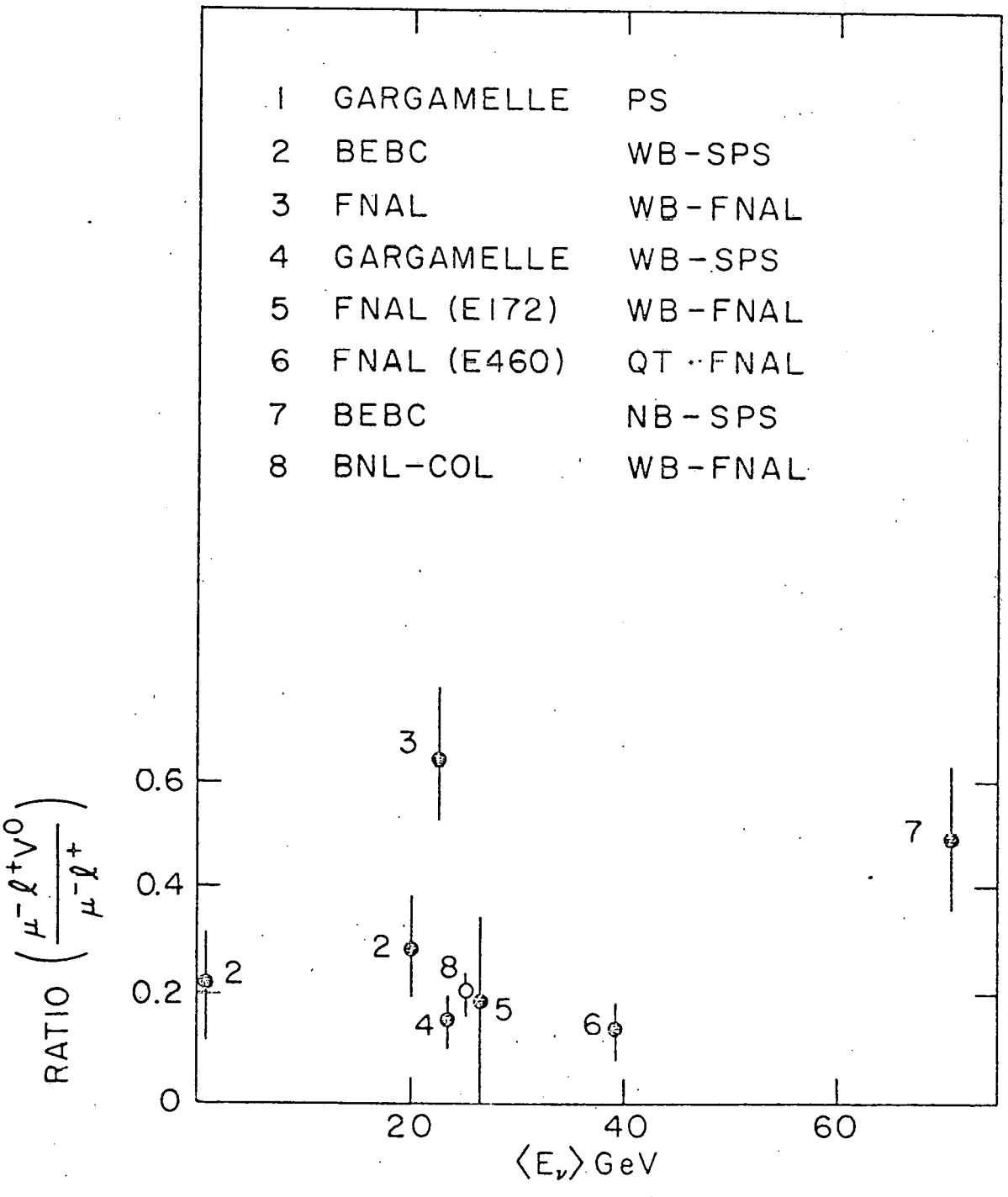

Fig. 3 Visible V^o content in various dilepton experiments.

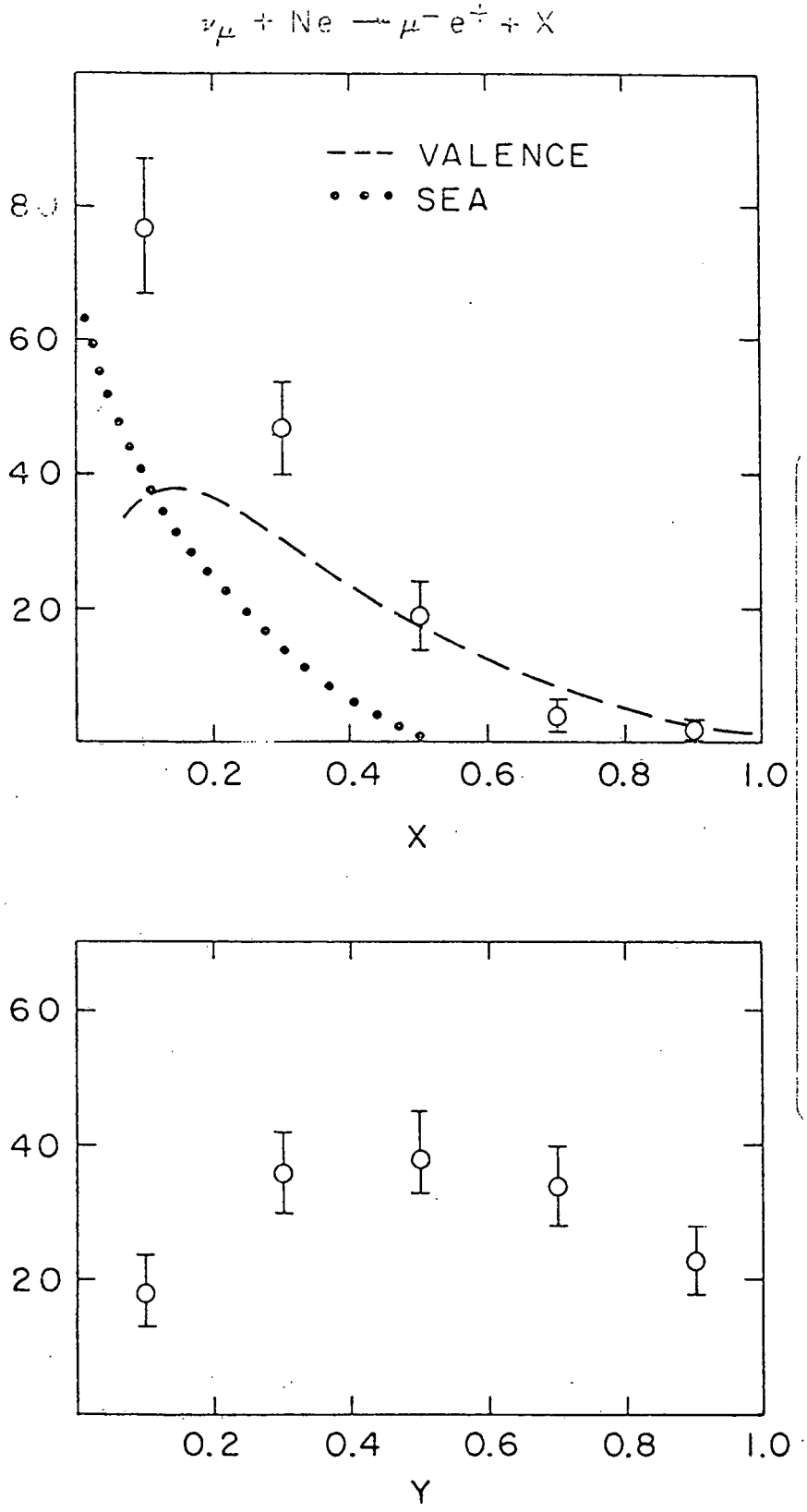

Fig. 4 X and Y variables for dilepton events. The curves represent fitted contributions from valence and sea quarks.

8-506-78

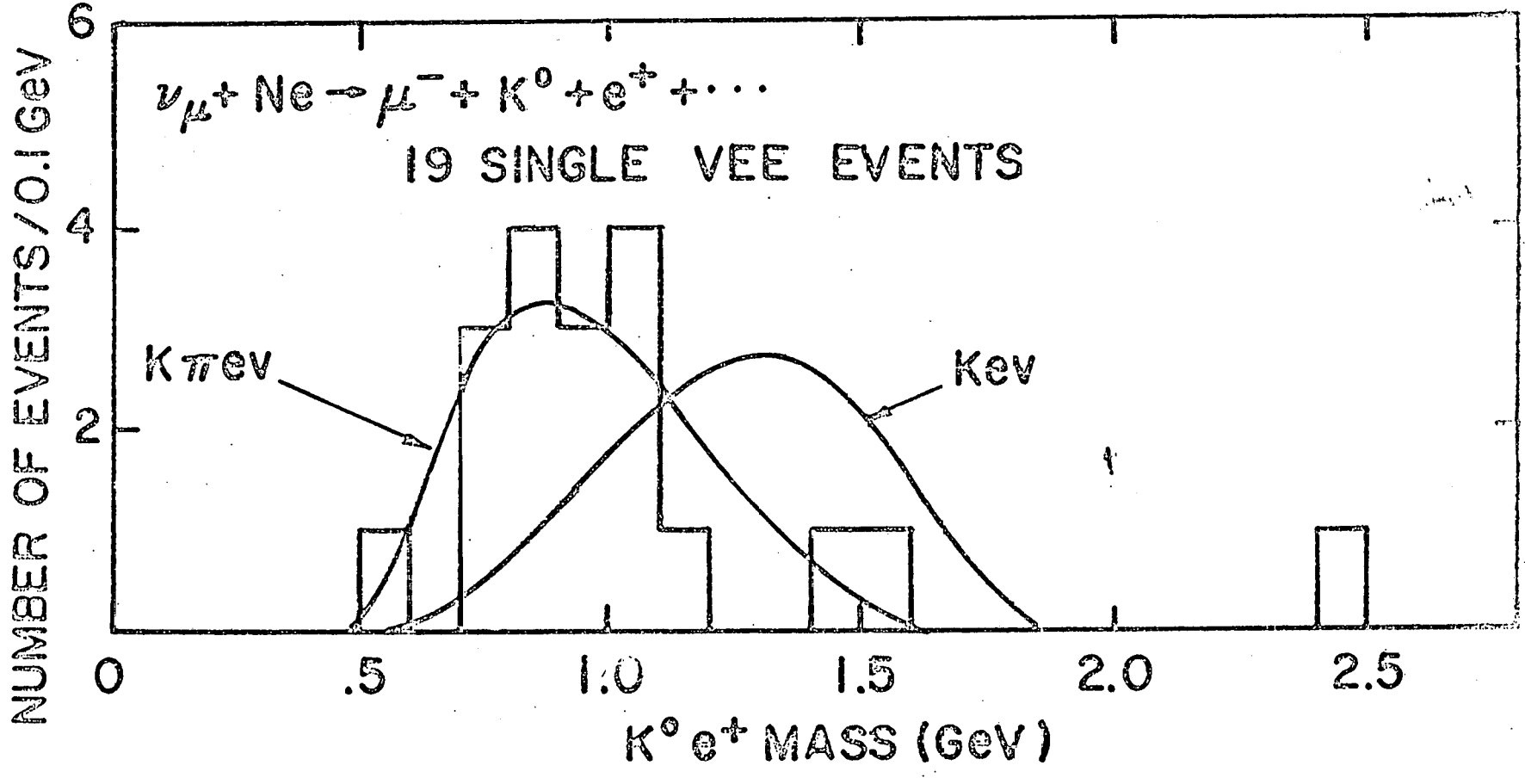

Fig. 5 K^0e^+ mass from dilepton sample.

with a single K^o. The data are not in good agreement with the distribution expected from the $K^o e^+ \nu_e$ decay of a spin zero D^+ meson at 1868 MeV. The distribution is consistent with a calculation by Barger et al.[17] assuming a $K\pi e\nu$ decay. However, 3-body decay modes are not excluded (the only 3-body D^o decay mode $D^o \to K^- e^+ \nu$ can not contribute to the plot).

b) By Antineutrinos

Recently two groups working at FNAL have presented results on dilepton production ($\mu^+ e^-$) by antineutrinos.[6,7] The statistics in each case (Table II) are low but the situation relative to neutrino produced dileptons is rather clear. The strange particle content is higher $\sim$ 0.5 ($K_S \to \pi^+\pi^- + \Lambda^o \to p\,\bar{\pi}$) per event which, when corrected for missing neutrals and with reasonable assumptions on the relative production of charged and neutral strange particles, yields $\sim$2 strange particles per event.[7] The x-distribution peaks at small x-values consistent with production from sea quarks. The rate is probably lower than for neutrino production of dileptons. In all cases the results are in accord with the expectations of the GIM charm model. However, it is clear that improved statistics will greatly facilitate the comparison with the model.

IV. Search for Non Leptonic Charm Decays

All events with possible vees ($K_s \to \pi^+\pi^-$ or $\Lambda^o \to p\pi^-$ decays) in about 80,000 pictures, corresponding to 46,000 charged current events with a muon momentum over 2 GeV/c, were measured. Good 2 or 3 constraint fits for 1815 $K_S \to \pi^+\pi^-$ and 1367 $\Lambda \to p\pi^-$ decays

TABLE II

μ^+e^- Events in Antineutrino Interactions

	Berkeley Hawaii-Seattle[6]	Fermilab-IHEP ITEP-Michigan[7]
$\bar{\nu} \to \mu^+$...Events	2800	6320
$\bar{\nu} \to \mu^+e^-$...Events	4	12
$\bar{\nu} \to \mu^+e^-V^o$ Events*	2	7
Rate μ^+e^-/μ^+...	$(0.15\ ^{+0.14}_{-0.08})\%$	$(0.22 \pm 0.07)\%$

*V^o stands for $K^o_s \to \pi^+\pi^-$ or $\Lambda^o \to p\pi^-$ decay associated with the primary vertex.

were obtained. Correcting for branching ratios and detection efficiencies, this corresponds to a $(K^o + \bar{K}^o)$ rate of $(13.6 \pm 1.5)\%$ of all charged current events, and a $(\Lambda^o + \Sigma^o)$ rate of $(5.0 \pm 0.5)\%$.

Figures 6a and 6b show the $K^o_S\pi^+$ and the $K^o_S\pi^+\pi^-$ mass distributions, respectively. There is a peak in the $K^o\pi^+\pi^-$ distribution in the mass region of the charmed D^o meson seen at SPEAR.[18] The best fit of a polynomial background plus a Gaussian, shown by the curve on Fig. 7a gives the following parameters:

$$M = 1850 \pm 15 \text{ MeV}, \quad \sigma = 20 \pm 8 \text{ MeV}$$

corresponding to 64 events above a background of 180, with a statistical significance of four standard deviations. The width is consistent with the experimental mass resolution of 20 MeV. No corresponding peak is apparent near the D mass in the events without a μ^- (Fig. 7b). This is consistent with the prediction of the GIM model that the charm charging neutral current interactions are absent. If the peak were due to K^* production, then one might expect it to be present in events with and without a μ^-.

Correcting for branching ratios and detection efficiencies, the measured rate is

$$\frac{\nu_\mu + Ne \to \mu^- + D^o + \ldots,\ D^o \to K^o\pi^+\pi^-}{\nu_\mu + Ne \to \mu^- + \ldots} = (0.7 \pm 0.2)\%.$$

There is no significant peak at the D^+ mass in the $K^o\pi^+$ mass distribution. Fitting to a Gaussian with the width of the mass resolution centered on the D^+ mass gives a result of 11 ± 8 $D^+ \to K^o\pi^+$ events, which is clearly not a significant signal. Using the branching ratios measured at SPEAR[19] of $4 \pm 1.3\%$ for

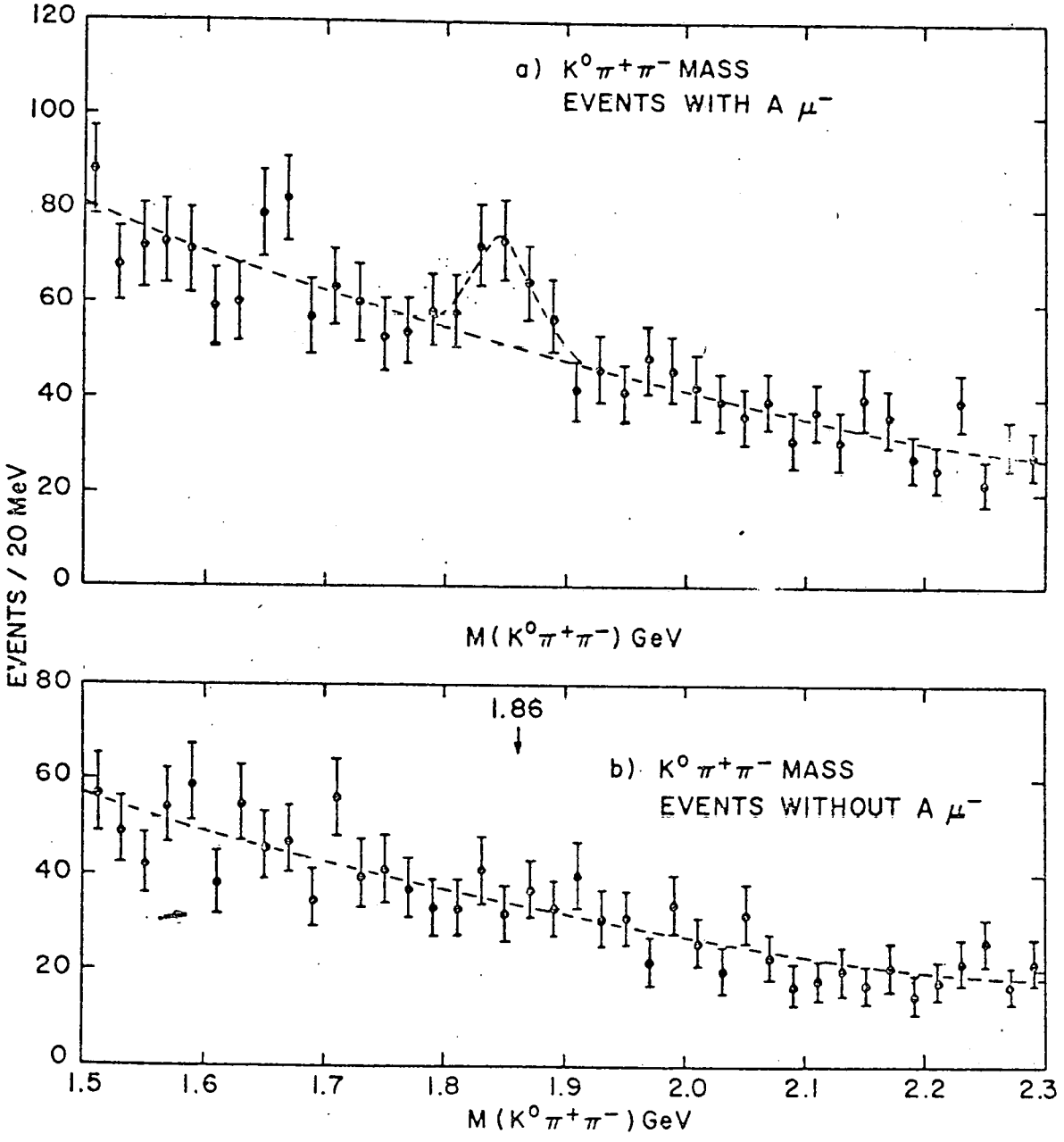

Fig. 6 $K^0\pi^+\pi^-$ invariant mass distributions for a) events with μ^- candidates; and b) events without μ^- candidates.

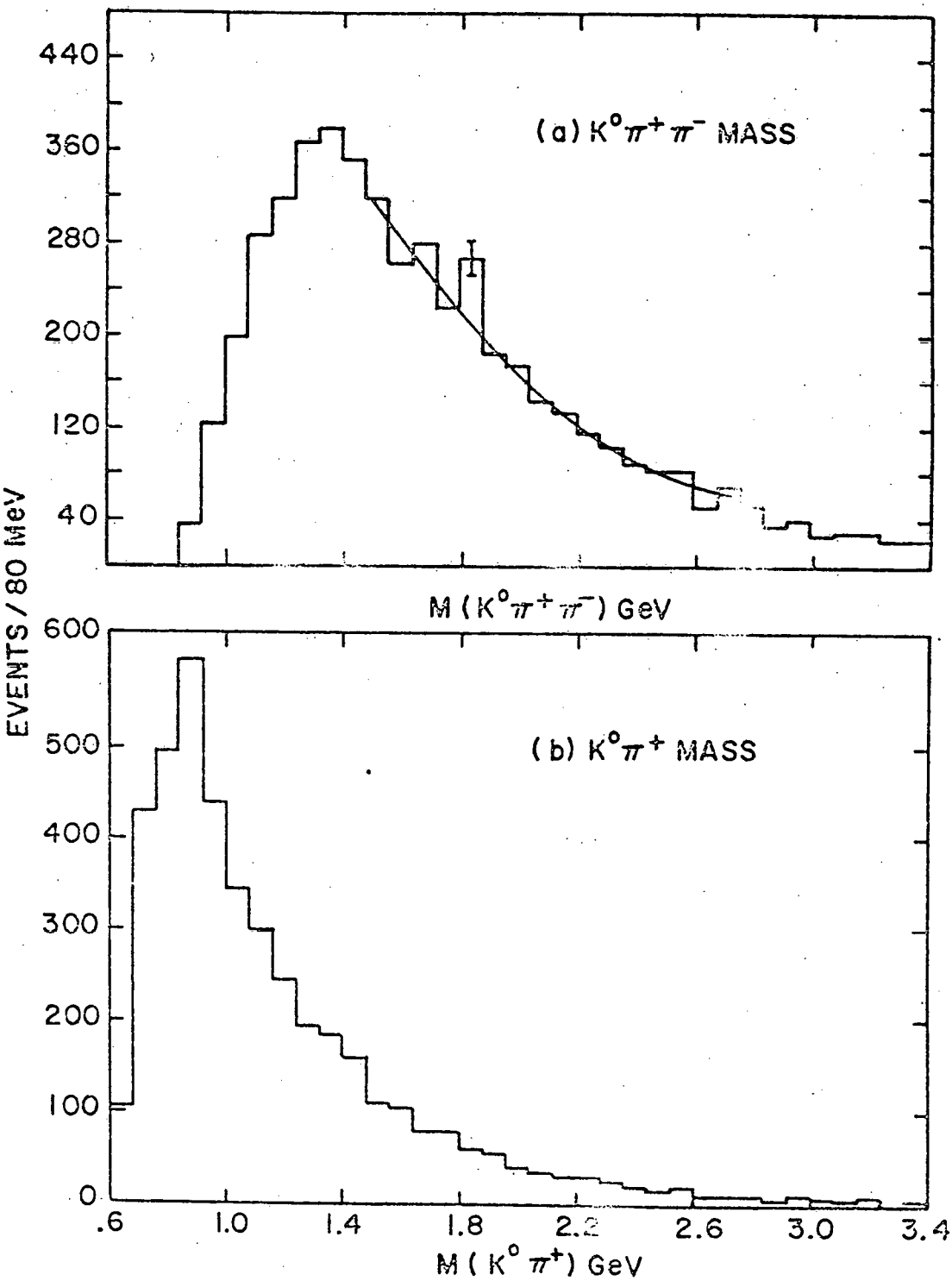

Fig. 7 a) $K^0\pi^+\pi^-$ and b) $K^0\pi^+$ invariant mass distributions from charged current events.

$D^o \to K^o\pi^+\pi^-$ and 1.5 ± 0.6% for $D^+ \to K^o\pi^+$, the ratio of D^+ to D^o production by neutrinos is $D^+/D^o = 0.5 \pm 0.4$.

The D^o rate can be compared with the previously measured rate for $\nu_\mu + Ne \to \mu^- + e^+ + .../\nu_\mu + Ne \to \mu^- + ...$ of (0.5 ± 0.15)%[2] It is not possible to obtain an exact value for the ratio of semileptonic to $K^o\pi^+\pi^-$ decays of the D^o since it is not known what fraction of the μ^-e^+ events come from D^o decays. If it is assumed that all of the μ^-e^+ events are due to semileptonic D^o decays, $D^o \to e^+ + ...$, then the ratio $R = (D^o \to e^+ + ...)/(D^o \to K^o\pi^+\pi^-)$ is $R = 0.7 \pm 0.3$. If, on the other hand, only a fraction of the μ^-e^+ events is due to D^o decays, which is more reasonable since there is likely to be some D^+ and charmed baryon decays contributing to the μ^-e^+ events, then the value for R is less than that given above. Recent measurements at SPEAR yield the branching ratios of (4.0 ± 1.3)% for $D^o \to K^o\pi^+\pi^-$,[19] and (7.2 ± 2.8)% for $D \to e^+ + ...$,[20] which correspond to a value of $R = 1.8 \pm 0.9$, assuming equal semileptonic branching ratios for the D^o and the D^+. The Brookhaven-Columbia values, with any assumption about the D^o contribution to the μ^-e^+ events, are lower than the SPEAR value for R. However, the errors on all of these numbers are rather large at the present.

V. Search for Charmed Baryons

There is an indication of charmed baryon production in the dilepton sample. Since 10 events of the type $\nu_\mu + Ne \to \mu^- + e^+ + \Lambda^o + ...$ are observed where about five events are expected from associated production. These Λ^o's can not come from D meson decay

nor from the $\bar{s}$ quark left over when the e^+ comes from charm produced on an s quark in the sea.

The hadronic decays of charmed baryons into Λ's were searched for. Figures 8a and 8b show the $\Lambda^o\pi^+$ and the $\Lambda^o\pi^+\pi^+\pi^-$ mass distribution from events of the type $\nu_\mu + Ne \rightarrow \mu^- + \Lambda^o$ + hadrons. There is no enhancement in the $\Lambda\pi^+\pi^+\pi^-$ mass at 2250 MeV. A small peak with 20 ± 9 events is present in the $\Lambda\pi^+$ mass at 2250 MeV but the signal is not present if a cut in helicity angle (require $\cos\theta^* > -0.6$) is made. This cut was chosen to remove a background of events with a slow Λ and a fast π and should have enhanced the Λ_c^+ signal to background. Thus, this is considered at this time to be a statistical fluctuation. From these results the 90% confidence level limit for $\Lambda_c^+ \rightarrow \Lambda\pi^+\pi^+\pi^-$ is $\leq$ 0.2% while the $\Lambda\pi^+$ signal, if real, leads to a rate for the $\Lambda_c^+ \rightarrow \Lambda\pi^+$ mode of (0.1 ± 0.5)%.

VI. $\nu_\mu - e^-$ Elastic Scattering

The observation of neutral current induced neutrino interactions gave strong support to the gauge theories unifying weak and electromagnetic interactions. Presently all neutrino-hadron neutral current interactions are consistent with the SU(2) x U(1) gauge model proposed by Weinberg[21] and Salam[22] with a Weinberg angle $\sin^2\theta_w \approx 1/4$. One of the theoretically most stringent tests of this theory is provided by the purely leptonic process, $\nu_\mu e^- \rightarrow \nu_\mu e^-$ which can proceed only via the weak neutral current interaction,

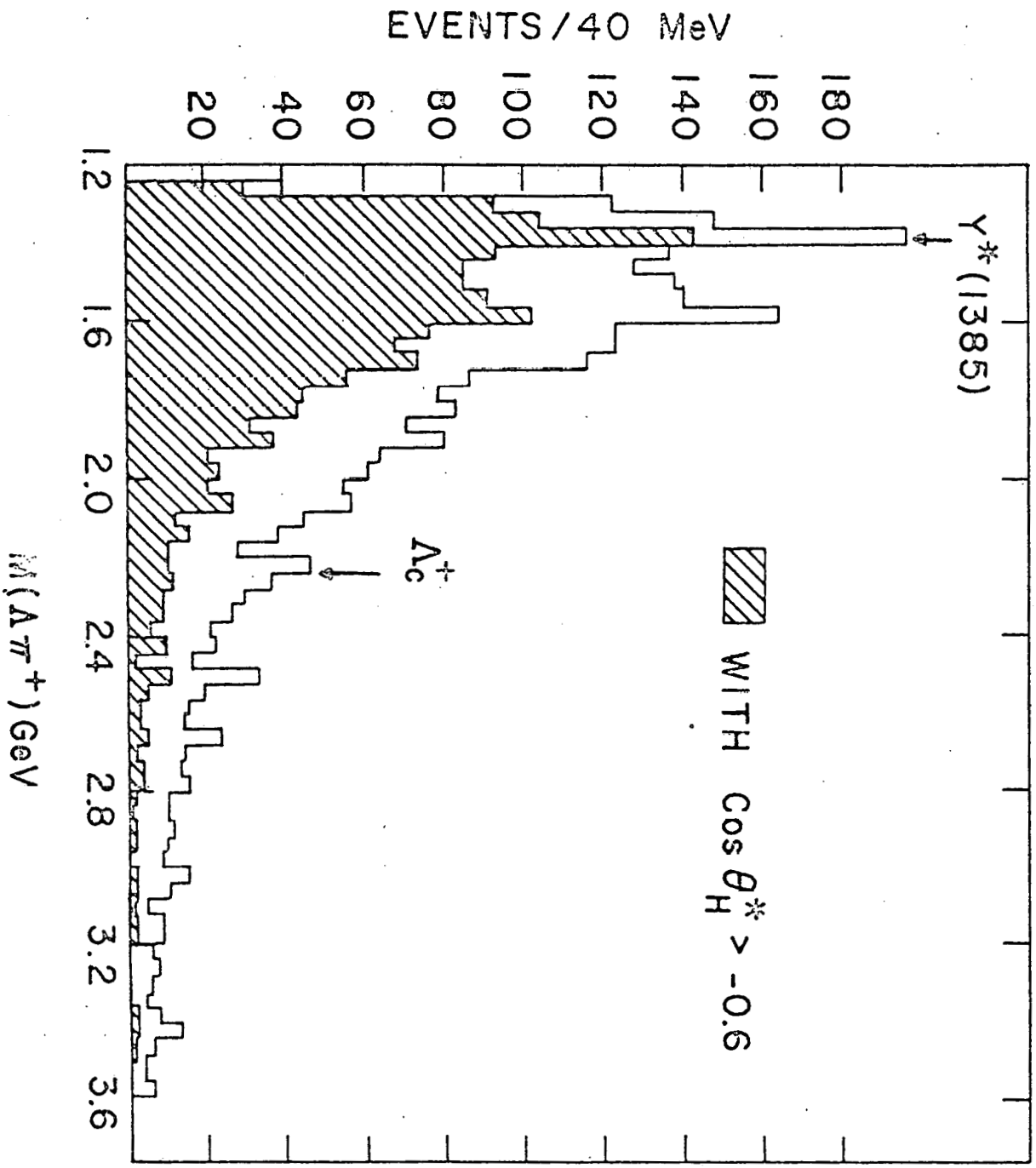

Fig. 8 a) $\Lambda\pi^+$ invariant mass distributions from charged current events.

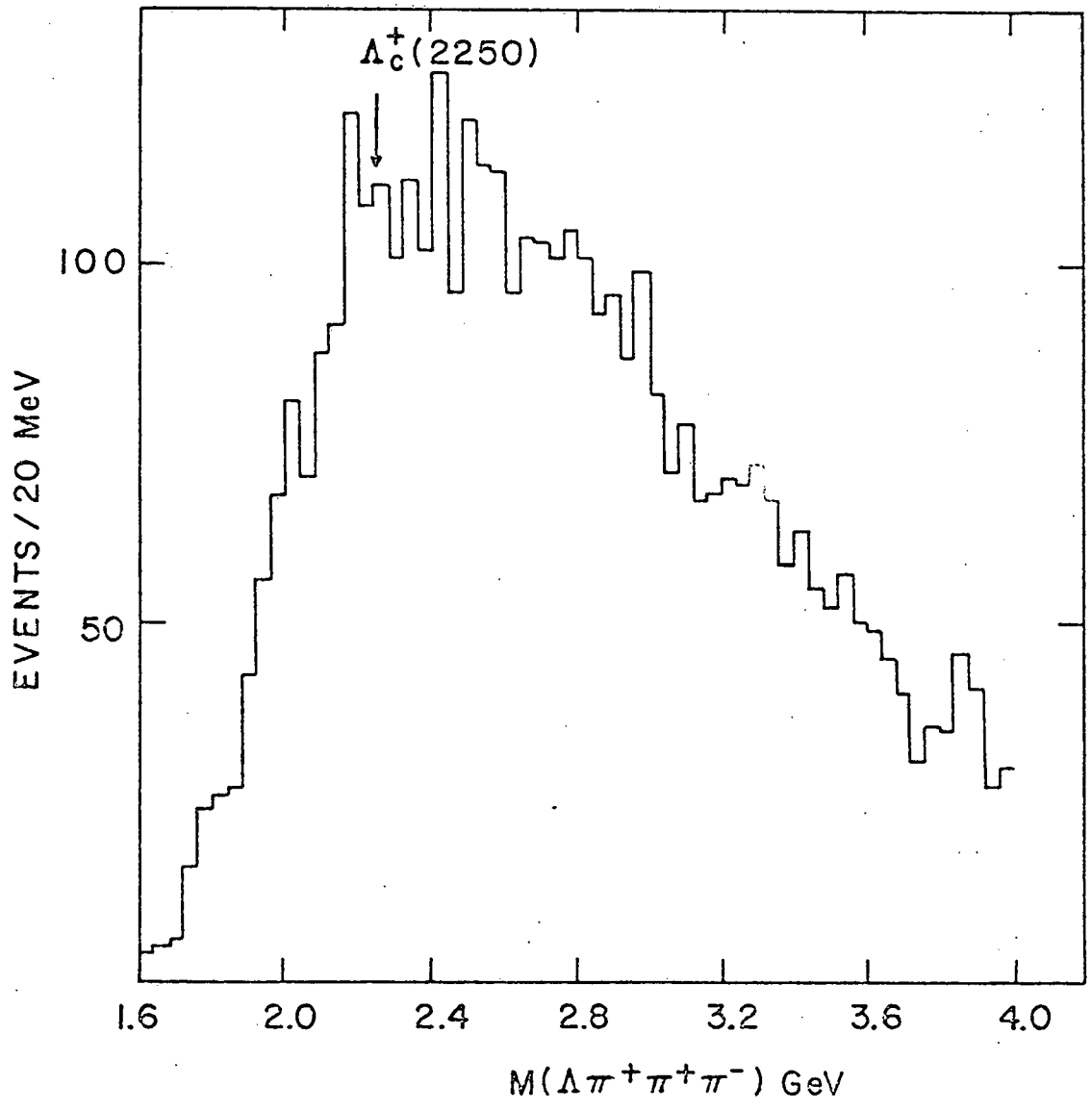

Fig. 8 b) $\Lambda\pi^+\pi^+\pi^-$ invariant mass distribution from charged current events.

and the theory can be compared to experimental measurement without uncertainties introduced by using hadronic targets. Early experimental results on this reaction at neutrino energies of a few GeV[23,24,25] are consistent with the Weinberg-Salam model. A recent result at higher energies[5] indicates a significantly higher cross section for this process than that expected from the Weinberg-Salam model. The Brookhaven-Columbia experiment, which has four times the charged current data sample, is in good agreement with the Weinberg-Salam model.

The entire data sample of 134,000 photographs containing 106,000 charged current ν_μ interactions was subjected to a dedicated scan for isolated electromagnetic showers; 93,000 of the pictures were double scanned. All forward energetic single e^-, single e^+, or $\gamma \rightarrow e^+e^-$ pairs with no other tracks originating at the interaction vertex were recorded. Electrons of either sign were identified by at least two signatures. All such events were examined by a physicist, measured, and geometrically reconstructed using the program, TVGP. By using the 93,000 double-scanned pictures the scanning efficiency was determined[26] to be (61 ± 15)% for a single scan, giving an overall scan efficiency of (78 ± 15)%.

Events which had energy $E \geq 2$ GeV and angle $\theta \leq 3^\circ$ and which were not associated with other events were retained for further consideration. The subsequent procedures adopted were guided by the philosophy of retaining single electron events and rejecting γ-ray conversions. An event was defined to be a single e^- if there was no visible radiation on a negative track before there was observable curvature so that the

event clearly had a single track at the origin. If there was early radiation within a short distance of the origin such that it was not possible to determine whether the event began as a single or double track (in all ambiguous cases this distance was less than 10 cm), then the event was still classified as a single e^- if, a) the fastest track was negative, b) the fastest positron coming from the confused region was less than 25% of the electron energy ($E^+/E^- < 1/4$), and c) the energy of the second fastest electron was greater than 10% of the positron energy. Condition (b) removes fast symmetric pairs while condition (c) obviates the problem of low energy δ rays on asymmetric pairs. In most instances the identification was clear cut; the spatial resolution and lack of confusion being sufficient to clearly distinguish among the noted categories. In three cases it was not possible to distinguish between a single e^- with early conversion and the production of a delta ray from a converted γ pair before clear separation of the lepton tracks. Adoption of the above rules relegated these three events to the γ category (two of the three are consistent with $\nu_\mu e^- \rightarrow \nu_\mu e^-$ kinematics). Corrections are made for real e^- events being classified as γ's by these procedures. The probability of an e^- radiating more than 1/4 of its energy in a single radiation within the first 10 cm sufficiently asymmetrical to be classified as a γ has been calculated to be 3%.

The final sample contains 11 unambiguous e^- events, 5 unambiguous e^+ events, and 22 γ pairs. The number of single e^+ events is quite consistent with what we expect from the reaction $\bar{\nu}_e p \rightarrow e^+ n$

induced by the small $\bar{\nu}_e$ contamination in the beam.[27] The energies and angles of the 11 single e^- events, listed in Table III, are compared to the kinematics of $\nu_\mu e^- \rightarrow \nu_\mu e^-$ scattering on Fig. 9. The curves show the expected correlation between E and θ of the electrons in the lab frame for E_ν = 30 GeV, the peak of our spectrum, and E_ν = 10 and 100 GeV, which are the approximate limits of our spectrum. All 11 e^- events are consistent with the kinematics of this reaction. The single e^+ and the γ events are not sharply peaked like the e^- events but are spread out up to the 52 mrad angle cut. An appropriate variable to illustrate this difference is $E\theta^2$, since the kinematic limit in $\nu_\mu e^- \rightarrow \nu_\mu e^-$ scattering, $E\theta^2 \leq 2\ m_e$ (electron mass) is independent of the incident neutrino or outgoing electron energies. The distributions in $E\theta^2$ for the e^-, e^+ and γ events are shown in Fig. 10. The e^- events are peaked below the $2\ m_e$ ($\sim$1 MeV) kinematic limit, while the e^+ and γ events are much more spread out.

Three sources of background that could produce single electrons in this experiment were considered:

a) Photons which Compton scatter or convert to e^+e^- pairs so asymmetrically that the e^+ is not seen are a negligible background. Another background comes from photons which convert into asymmetric e^+e^- pairs and have an early energetic δ so as to be classified as an e^- and not as a γ by the criteria noted above. The probability for this is calculated to be $\sim$1%. When multiplied by the total number of unassociated γ's that are consistent with the kinematics of $\nu_\mu e^- \rightarrow \nu_\mu e^-$ (8 events with $E\theta^2 < 3$ MeV) this yields .08 events which is negligible.

TABLE III

List of $\nu_\mu + e^- \rightarrow \nu_\mu + e^-$ Events

Event	E_{e^-} (GeV)	θ_{e^-} (mrad)	$E\theta^2$ (MeV)
1	3.7 ± 1.6	10 ± 5	0.4
2	4.7 ± 0.3	5 ± 8	0.1
3*	5.6 ± 2.6	5 ± 7	0.1
4	6.5 ± 1.6	8 ± 4	0.4
5*	8.8 ± 1.7	4 ± 3	0.1
6	9.0 ± 1.0	8 ± 5	0.6
7	14.0 ± 3.0	14 ± 10	2.7
8*	15.8 ± 2.6	8 ± 5	1.0
9	20.8 ± 5.6	2 ± 3	0.1
10	27.5 ± 9.0	8 ± 4	1.8
11	34.6 ± 4.0	4 ± 4	0.6

*Event out of fiducial volume used for the cross section calculation.

9-1312-78

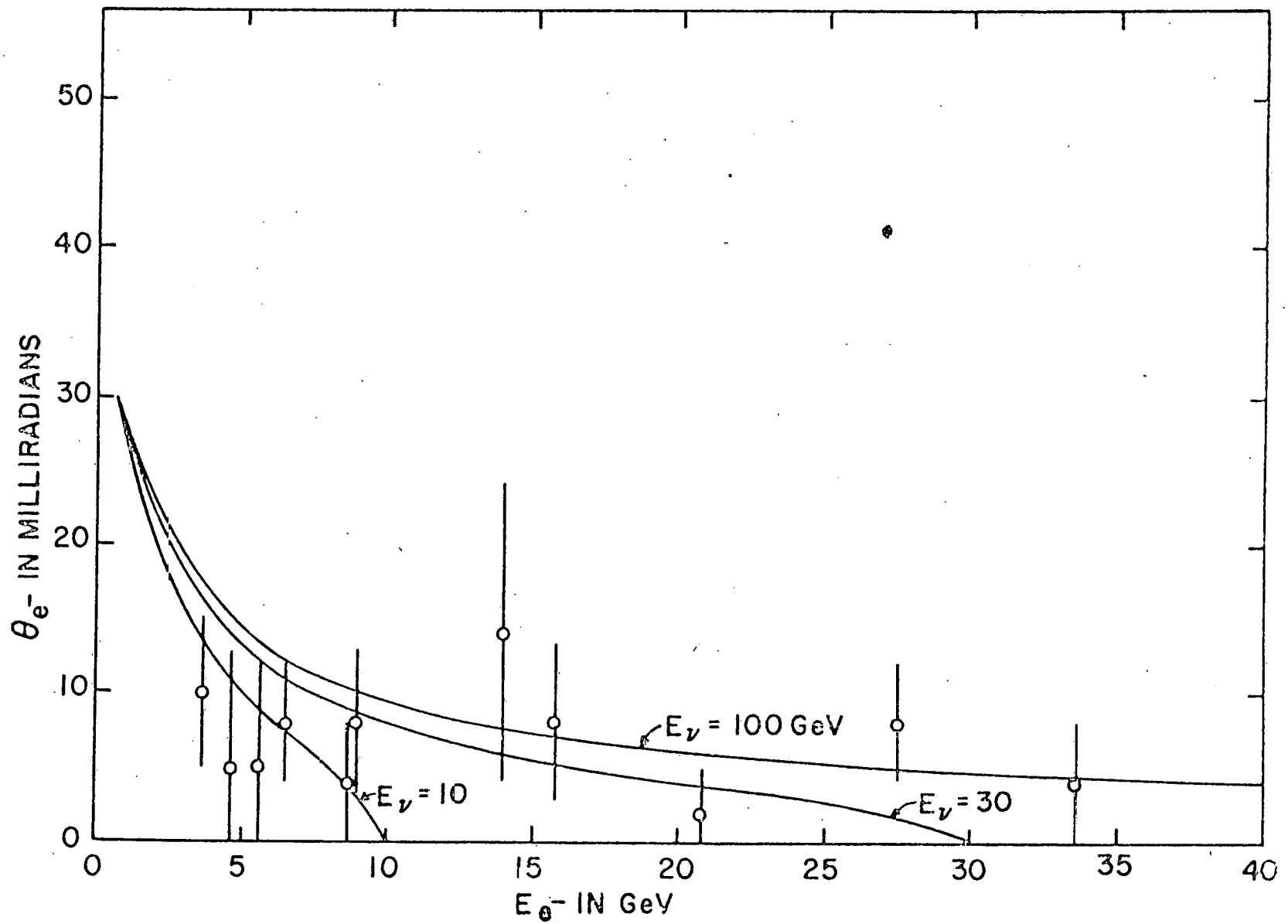

Fig. 9 Electron angle vs. energy of the 11 observed single electron events compared to the kinematics of the reaction $\nu_\mu e^- \rightarrow \nu_\mu e^-$ for various neutrino energies E.

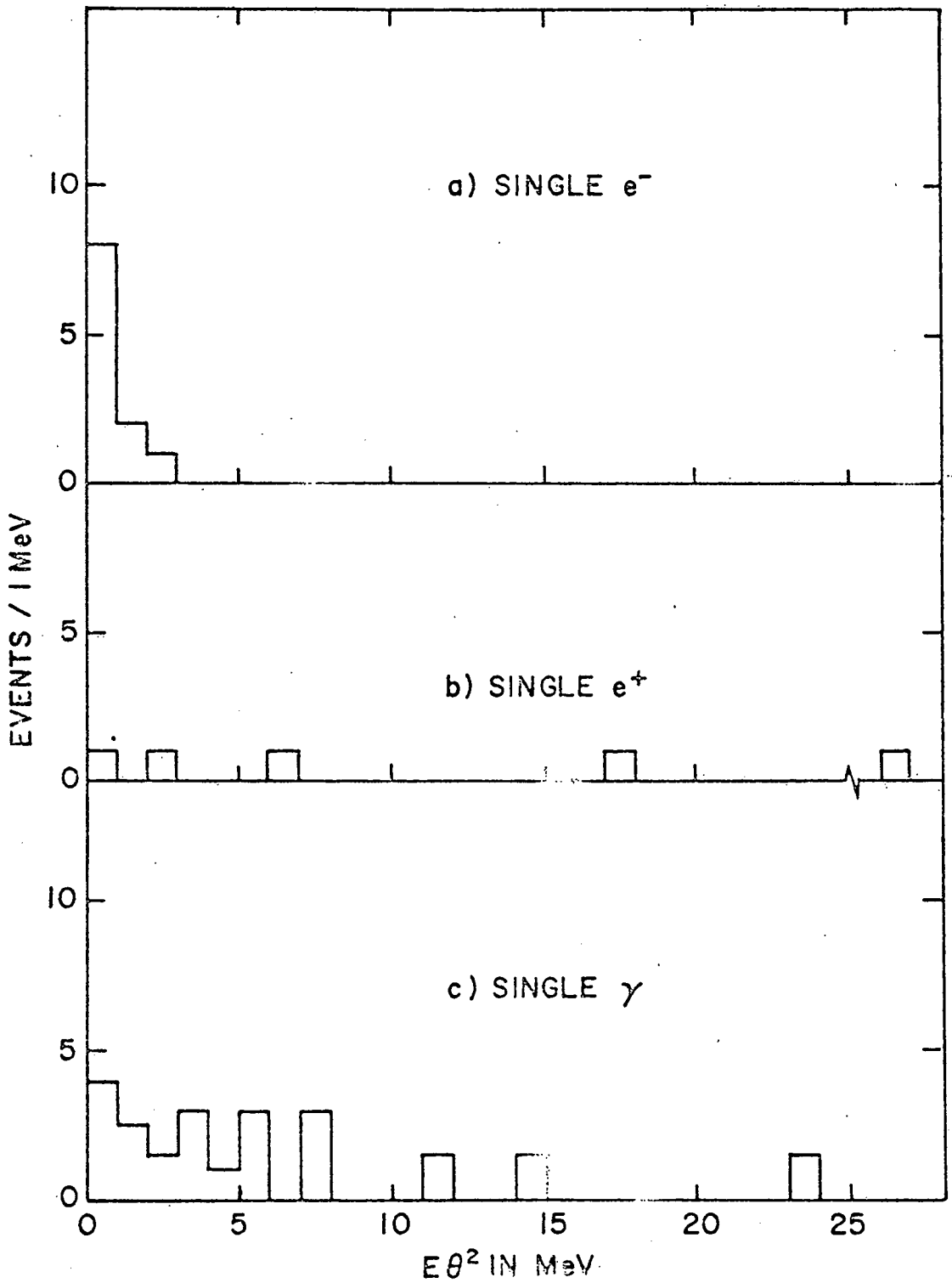

Fig. 10 Distribution in the variable $E\theta^2$ for a) the single e^- events; b) the single e^+ events; and c) the single $\gamma \rightarrow e^+e^-$ pairs.

b) The process $\nu_e n \to e^- p$ and $\nu_e n \to e^- p\pi^o$, where the proton is too low in energy to be seen, and the γ's from the π^o are mixed in with the shower of the e^-. In this experiment, they also scanned for and measured events with an e^- and hadrons,[27] and found 22 events with an e^- and a proton (with additional stubs which could be nuclear fragments) and possibly γ's from a π^o. From the expected q^2 distributions for these events, it was calculated[28] that 3% of these events would have an invisible proton and an e^- at a small enough angle to be consistent with the kinematics of $\nu_\mu e^- \to \nu_\mu e^-$. This background is calculated to be 0.7 events or (6 ± 6)% of the $\nu_\mu e^- \to \nu_\mu e^-$ signal.

c) The reactions $\bar{\nu}_\mu e^- \to \bar{\nu}_\mu e^-$, $\nu_e e^-$, and $\bar{\nu}_e e^- \to \bar{\nu}_e e^-$ are indistinguishable from the $\nu_\mu e^- \to \nu_\mu e^-$ reaction. However, since the relative fluxes in the beam are $\nu_\mu/\bar{\nu}_\mu/\nu_e/\bar{\nu}_e \simeq 100/3/1/0.1$, the contribution of these reactions in any reasonable model is expected to be small in this experiment.

The 11 $\nu_\mu e^- \to \nu_\mu e^-$ events and the corresponding 106,000 charged current ν_μ interactions are in a volume visible to all three cameras. To calculate the cross section for this process, one imposes a more restricted fiducial volume to insure a uniform (and essentially 100%) detection efficiency for high energy electrons.[29] Then 8 of the 11 $\nu_\mu e^- \to \nu_\mu e^-$ events and 79% of the charged current ν_μ interactions are in this fiducial volume. After subtracting (6 ± 6)% for the $\nu_e n \to e^- p$ background, correcting for the (78 ± 15)% scan efficiency, and for the following losses of single electrons: 10% for the 2 GeV cut[30] on E_e, 3% for loss of e^- classified as γ, and 3% miscellaneous losses such as a false association with another

ν event etc., one obtains the ratio

$$\frac{\nu_\mu + e^- \rightarrow \nu_\mu + e^-}{\nu_\mu + Ne \rightarrow \mu^- + \ldots} = (1.36 \pm 0.54) \times 10^{-4}.$$

One can calculate the total cross section for this process by using the total charged current cross section $\sigma_{tot} = (0.67 \pm 0.06) \times 10^{-38} E_\nu$ cm^2/nucleon measured in the energy range of 20 to 60 GeV in a BEBC experiment[31] and by noting that the electron to total nucleon ratio in neon is 1/2. The result is

$$\sigma(\nu_\mu + e^- \rightarrow \nu_\mu + e^-) = (1.8 \pm 0.8) \times 10^{-42} E_\nu \text{ cm}^2$$

where E_ν is the incident neutrino energy in units of GeV.

This result is in disagreement with a recent measurement in the GARGAMELLE experiment[5] at the CERN SPS. On the other hand, our result is in good agreement with the Weinberg-Salam model. Figure 11a shows a comparison of the results with the prediction of the model as a function of the mixing angle $\sin^2\theta_w$. The data restrict the value of $\sin^2\theta_w$ to be $0.20^{+.16}_{-.08}$ or $0.57^{+.07}_{-.17}$, the former value being in excellent agreement with several previous neutral current measurements.[32] Figure 3b shows the energy distribution of the 11 $\nu_\mu e^- \rightarrow \nu_\mu e^-$ events. The curve on the figure is the prediction of the Weinberg-Salam model with $\sin^2\theta_w = .25$ integrated over the incident neutrino energy spectrum. The agreement is quite good.

This research was supported by the U.S. Department of Energy and the National Science Foundation.

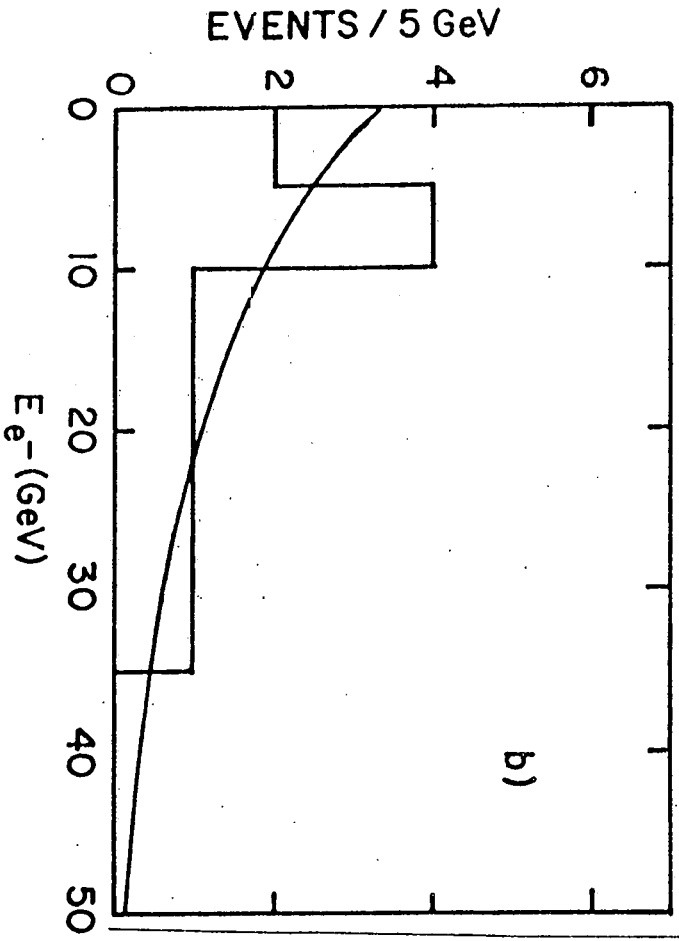

Fig. 11 b) Distribution in the electron energy of the 11 $\nu_\mu e^- \to \nu_\mu e^-$ events. The curve is the prediction of the Weinberg-Salam model with $\sin^2\theta_w = 1/4$ integrated over the incident neutrino energy spectrum of the experiment.

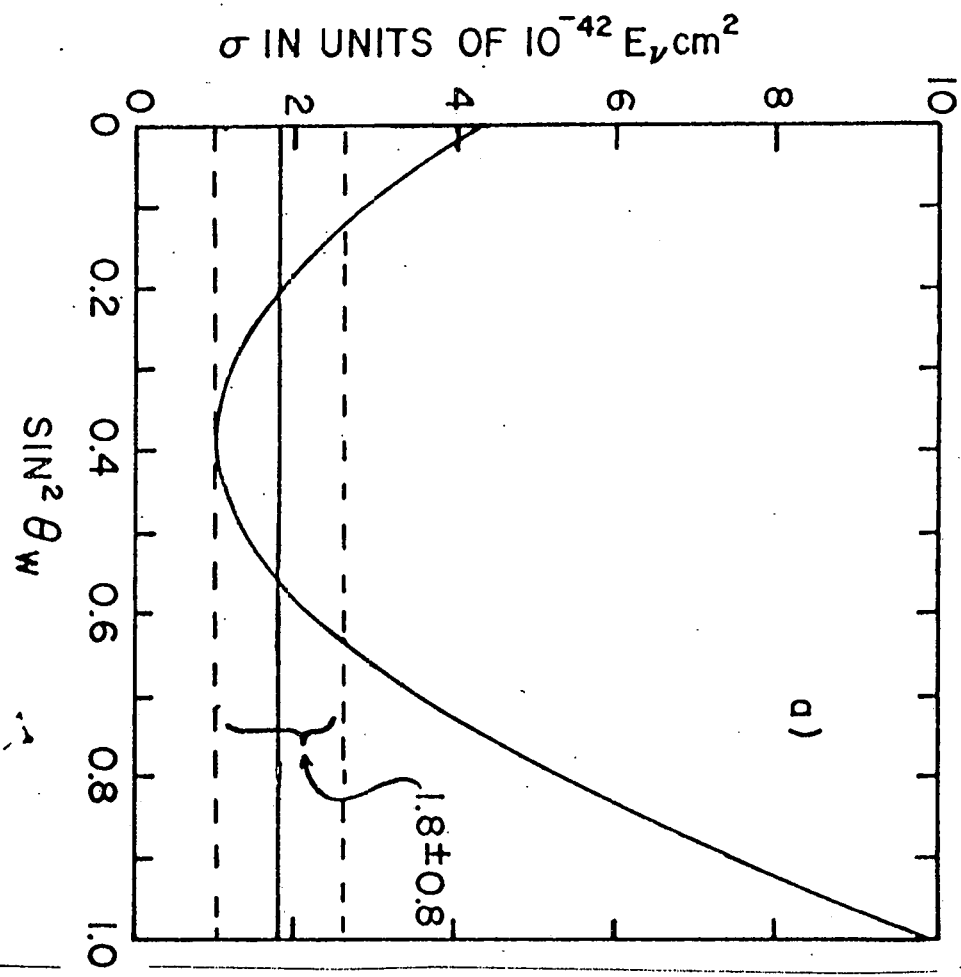

Fig. 11 a) Comparison of the prediction of the Weinberg-Salam model with the measured cross section for $\nu_\mu e^- \to \nu_\mu e^-$.

References

1. Brookhaven National Laboratory-Columbia University Group:

   A.M. Cnops, P.L. Connolly, S.A. Kahn, H.G. Kirk, M.J. Murtagh, R.B. Palmer, N.P. Samios and M. Tanaka, Brookhaven National Laboratory, Upton, N.Y. 11973
   C. Baltay, D. Caroumbalis, H. French, M. Hibbs, R. Hylton, M. Kalelkar and W. Orance, Columbia University, New York, N.Y. 10027.

2. C. Baltay et al., Phys. Rev. Lett. 39, 62 (1977).

3. C. Baltay et al., Phys. Rev. Lett. 41, 73 (1978).

4. A.M. Cnops et al., Phys. Rev. Lett. 41, 357 (1978).

5. P. Alibran et al., Phys. Lett. 74B, 422 (1978).

6. H.C. Ballagh et al., Phys. Rev. Lett. 39, 1650 (1977).

7. J.P. Berge et al., Submitted to Phys. Rev. Lett.

8. A. Benvenuti et al., Phys. Rev. Lett. 34, 419 (1975).

9. S.L. Glashow, J. Iliopoulos, L. Maiani, Phys. Rev. D2, 1285 (1970).

10. Associated charm production will yield $\mu^- e^-$ ($\mu^+ e^+$) events in neutrino (antineutrino) interactions. Since there is no significant bubble chamber data on these final states no discussion of associated charm production is included.

11. H. Deden et al., Phys. Lett. 67B, 474 (1977).

12. P. Bosetti et al., Phys. Rev. Lett. 38, 1248 (1977).

13. F. Harris, Presented at Topical Conference on Neutrino Physics at Accelerators, Oxford University, England, July 3-7, 1978.

14. P.C. Bosetti et al., Phys. Lett. 73B, 380 (1978).

15. O. Erriquez et al., Phys. Lett. 77B, 227 (1978).

16. A. Blondel, Presented at Topical Conference on Neutrino Physics at Accelerators, Oxford University, England, July 3-7, 1978.

17. V. Barger et al., Phys. Rev. D16, 746 (1977).

18. G. Goldhaber et al., Phys. Rev. Lett. 37, 255 (1976).

19. I. Peruzzi et al., Phys. Rev. Lett. 39, 1301 (1977).

20. J.M. Feller et al., Phys. Rev. Lett. 40, 274 (1978). There have been other results on the semileptonic branching ratio (W. Bacius et al., Phys. Rev. Lett. 40, 671 and R. Brandelik et al., Phys. Lett. 70B, 387). We use the results of J.M. Feller et al. since they were obtained in the same experiment as the $K\pi\pi$ branching ratio of Ref. 18.

21. S. Weinberg, Phys. Rev. Lett. 19, 1264 (1967).

22. A. Salam, in Elementary Particle Theory, N. Swartholm, Ed. (Stockholm 1969).

23. F.J. Hasert et al., Phys. Lett. 46B, 131 (1973); J. Blietschau et al., Nucl. Phys. B114, 189 (1976).

24. J. Blietschau et al., Phys. Lett. 73B, 232 (1978).

25. H. Faissner et al., Phys. Rev. Lett. 41, 213 (1978).

26. To determine the scan efficiency a sample of 134 high energy forward e^+, e^-, and γ's was used. The result is consistent with an (86 ± 20)% efficiency obtained from the 11 single e^- events alone.

27. In a sample of 27,600 total $\nu_\mu \to \mu^-$ interactions, 187 ± 14 and 28 ± 6 total $\nu_e \to e^-$ and $\bar{\nu}_e \to e^+$ interactions, respectively, were found (A. Cnops et al., Phys. Rev. Lett. 40, 144). Scaling these numbers by 106,000/27,600 one obtains 723 ± 54 and 108 ± 23 total ν_e and $\bar{\nu}_e$ interactions, respectively, in the present sample. From these numbers there should be 15 $\nu_e n \to e^- p$ and 6 $\bar{\nu}_e p \to e^+ n$ events, consistent numbers actually seen.

28. This estimate is in good agreement with the measurement in the GARGAMELLE experiment of R_μ = (μ^- within 3°) (proton unseen)/ (μ^- + p) = (5 ± 3)%, assuming $\nu_e - \nu_\mu$ universality. ibid Ref. 5.

29. The fiducial volume is defined by $R \leq 170$ cm, $|z| \leq 125$ cm, and $D \geq 78$ cm, where R is the distance from the center of the chamber, z is the vertical distance from the median plane, and D is the distance from the back wall of the chamber along the beam direction.

30. The 10% loss due to the $E_e \geq 2$ GeV cut was calculated using the Weinberg-Salam model with a $\sin^2\theta_w = 1/4$. However, this loss is only weakly dependent on the model used.

31. K. Schultze, Proceedings of the Symposium on Lepton and Photon Interactions, p. 359. Hamburg (1977).

32. M. Holder et al., Phys. Lett. 71B, 222 (1977); B.C. Barish et al., Proceedings of the International Neutrino Conference, Aachen 1976, 289; P. Wanderer et al., Phys. Rev. D17, 1679 (1978).